

Residual-ZZ-coupling suppression and fast two-qubit gate for Kerr-cat qubits based on level-degeneracy engineering

Takaaki Aoki,^{1, a)} Akiyoshi Tomonaga,^{1, 2} Kosuke Mizuno,¹ and Shumpei Masuda^{1, 2, b)}

¹⁾Global Research and Development Center for Business by Quantum-AI Technology (G-QuAT), National Institute of Advanced Industrial Science and Technology (AIST), 1-1-1 Umezono, Tsukuba, Ibaraki 305-8568, Japan

²⁾NEC-AIST Quantum Technology Cooperative Research Laboratory, National Institute of Advanced Industrial Science and Technology (AIST), 1-1-1 Umezono, Tsukuba, Ibaraki 305-8568, Japan

(Dated: 2 October 2024)

Building large-scale quantum computers requires an interqubit-coupling scheme with a high on-off ratio to avoid unwanted crosstalk coming from residual coupling and to enable fast multi-qubit operations. We propose a ZZ-coupling scheme for two Kerr-cat qubits with a frequency-tunable coupler. By making four relevant states of the two Kerr-cat qubits quadruply degenerate, we can switch off the ZZ coupling. By partially lifting the level degeneracy, we can switch it on. We theoretically show that an experimentally feasible circuit model suppresses the residual ZZ coupling. Moreover, our circuit can realize $R_{ZZ}(-\pi/2)$ -gate fidelity higher than 99.999% within 25 ns when decoherence is ignored.

A Kerr-cat qubit, which stores quantum information on a squeeze-driven Kerr-nonlinear oscillator,^{1–3} is attracting much attention as a candidate platform for quantum computation. One of its advantages is its biased-noise nature, namely long lifetime and moderate dephasing time,⁴ which allows efficient quantum error corrections.⁵ A universal gate set for Kerr-cat qubits can be constructed for example by Z-axis rotations (R_Z gates) with all rotation angles, an X-axis rotation (R_X gate) with rotation angle $-\pi/2$, and a ZZ rotation (R_{ZZ} gate) with rotation angle $-\pi/2$.² Various schemes for gate operations on Kerr-cat qubits have been studied: an R_Z gate with a single-photon drive;^{2,3} an R_X gate by controlling the oscillator frequency;^{2,3} an R_X gate using time evolution under the Kerr Hamiltonian without the squeezing drive;^{3,6} an R_X gate using effective excited states;⁷ an R_{ZZ} gate using beam-splitter coupling;^{2,3} an R_{ZZ} gate by controlling the phase of the squeezing drive;⁸ an R_{ZZ} gate using conditional driving;⁹ acceleration of the elementary gates;¹⁰ nontrivial bias-preserving gates.^{11–13} R_Z and R_X gates have been experimentally implemented.^{6,14}

An R_{ZZ} gate is based on ZZ coupling between qubits. If we cannot switch off the ZZ coupling, the residual coupling causes crosstalk¹⁵ among qubits, yielding unwanted correlations between them. Because crosstalk errors are difficult to remove with quantum error corrections, which in general depend on errors to be local,¹⁵ a scheme without residual coupling is desired to build a large-scale quantum computer. In order to suppress residual coupling, tunable couplers have been utilized in transmon systems,^{16–28} which also enable fast multi-qubit operations. In Ref. 29, the authors have developed a coupling scheme for two Kerr-cat qubits in which two tunable resonators are used as couplers and the frequency of a resonator is controlled. Although the scheme can suppress the residual coupling, a simpler scheme with less residual coupling is desirable.

In this Letter we propose a coupling scheme for two Kerr-cat qubits with a better performance using a single tunable resonator as a coupler. By tuning the coupler frequency, we engineer the degeneracy of four relevant states of the two Kerr-cat qubits. This allows a cancellation of the residual ZZ coupling and a fast and high-fidelity R_{ZZ} gate. We show a circuit model that is experimentally feasible and numerically investigate its performance.

Before discussing the scheme for Kerr-cat qubits, we explain the relation between ZZ coupling and energy-level degeneracy of a diagonalized two-qubit Hamiltonian. The Hamiltonian is given by

$$\hat{H}_{2q} = \sum_{l,m=0}^1 E_{l,m} |\psi_{l,m}\rangle \langle \psi_{l,m}| = \begin{pmatrix} E_{0,0} & 0 & 0 & 0 \\ 0 & E_{0,1} & 0 & 0 \\ 0 & 0 & E_{1,0} & 0 \\ 0 & 0 & 0 & E_{1,1} \end{pmatrix}, \quad (1)$$

where $\{|\psi_{l,m}\rangle | l, m \in \{0, 1\}\}$ are four eigenstates and form an orthonormal basis; $E_{l,m}$ is the eigenenergy of eigenstate $|\psi_{l,m}\rangle$. This Hamiltonian can be rewritten as

$$\hat{H}_{2q}/\hbar = \frac{\zeta_{II}}{4} \hat{I}\hat{I} + \frac{\zeta_{ZZ}}{4} \hat{Z}\hat{Z} + \frac{\zeta_{ZI}}{4} \hat{Z}\hat{I} + \frac{\zeta_{IZ}}{4} \hat{I}\hat{Z}, \quad (2)$$

where

$$\hbar\zeta_{II} = E_{0,0} + E_{0,1} + E_{1,0} + E_{1,1}, \quad (3)$$

$$\hbar\zeta_{ZZ} = E_{0,0} - E_{0,1} - E_{1,0} + E_{1,1}, \quad (4)$$

$$\hbar\zeta_{ZI} = E_{0,0} + E_{0,1} - E_{1,0} - E_{1,1}, \quad (5)$$

$$\hbar\zeta_{IZ} = E_{0,0} - E_{0,1} + E_{1,0} - E_{1,1}, \quad (6)$$

$$\hat{I} = \begin{pmatrix} 1 & 0 \\ 0 & 1 \end{pmatrix}, \quad \hat{Z} = \begin{pmatrix} 1 & 0 \\ 0 & -1 \end{pmatrix}, \quad (7)$$

and $\hbar = h/(2\pi)$ is the reduced Planck constant. ζ_{ZZ} in Eq. (4) is a ZZ-coupling strength.^{18–28} Our strategy to cancel ZZ coupling, $\zeta_{ZZ} = 0$, is to make the four eigenstates quadruply degenerate by tuning system parameters, which

^{a)}Electronic mail: takaaki-aoki@aist.go.jp

^{b)}Electronic mail: shumpei.masuda@aist.go.jp

also leads to $\zeta_{ZI} = 0$ and $\zeta_{IZ} = 0$. We define four logical states $\{\lvert \widetilde{l,m} \rangle \mid l,m \in \{0,1\}\}$ as the quadruply degenerate eigenstates.

On the other hand, if we retain the degeneracy between $\lvert \psi_{0,0} \rangle$ and $\lvert \psi_{1,1} \rangle$ and that between $\lvert \psi_{0,1} \rangle$ and $\lvert \psi_{1,0} \rangle$ while partially lifting the degeneracy between the former two states and the latter two, we can perform only an R_{ZZ} gate as follows. We assume that at $t = 0$, ZZ coupling is switched off, $\zeta_{ZZ}(0) = 0$. We prepare the initial state as

$$\lvert \Psi(0) \rangle = \sum_{l,m=0}^1 \beta_{l,m} \lvert \widetilde{l,m} \rangle, \quad (8)$$

where $\beta_{l,m}$ is a coefficient. When the system parameters are changed adiabatically with the condition $\zeta_{ZZ}(t_g) = 0$, where t_g is the gate time, the state of the system at $t = t_g$ becomes

$$\begin{aligned} \lvert \Psi(t_g) \rangle &= \mathcal{T} \left[\exp \left(-\frac{i}{\hbar} \int_0^{t_g} \hat{H}_{2q}(t) dt \right) \right] \lvert \Psi(0) \rangle \\ &= e^{-i\theta} \hat{R}_{ZZ}(\Theta) \lvert \Psi(0) \rangle =: e^{-i\theta} \lvert \Psi_\Theta^{\text{ideal}} \rangle, \end{aligned} \quad (9)$$

where \mathcal{T} is the time-ordering operator,

$$\theta := \int_0^{t_g} \frac{\zeta_{II}(t)}{4} dt \quad (10)$$

is a global phase, and

$$\begin{aligned} \hat{R}_{ZZ}(\Theta) &= \sum_{l,m=0}^1 e^{-i(2\delta_{l,m}-1)\Theta/2} \lvert \widetilde{l,m} \rangle \langle \widetilde{l,m} \rvert \\ &= \begin{pmatrix} e^{-i\Theta/2} & 0 & 0 & 0 \\ 0 & e^{i\Theta/2} & 0 & 0 \\ 0 & 0 & e^{i\Theta/2} & 0 \\ 0 & 0 & 0 & e^{-i\Theta/2} \end{pmatrix} \end{aligned} \quad (11)$$

with

$$\Theta := \int_0^{t_g} \frac{\zeta_{ZZ}(t)}{2} dt \quad (12)$$

being the rotation angle and $\delta_{l,m}$ being the Kronecker delta. Here, we have ignored decoherence. In reality, some unwanted nonadiabatic transitions are unavoidable, and the second equal sign in Eq. (9) is replaced by an approximately equal one. For evaluation of the degree of approximation, we later calculate the average gate fidelity³⁰ (see Sec. I in the supplementary material for its definition). We show a schematic of our level-degeneracy engineering in Fig. 1.

Now, we introduce the level-degeneracy engineering for Kerr-cat qubits. We consider a system consisting of two Kerr parametric oscillators^{2,3} (KPOs, subsystems 1 and 2) and a tunable resonator (subsystem c). This system constitutes two Kerr-cat qubits. A circuit model of our system is shown in Fig. 2. The center of each SQUID of subsystem $\lambda \in \{1, 2, c\}$ is threaded by a magnetic flux $\tilde{\Phi}_\lambda(t)$. We decompose a dimensionless magnetic flux $\tilde{\varphi}_\lambda(t) := \tilde{\Phi}_\lambda(t)/\phi_0$, where $\phi_0 = \hbar/(2e)$

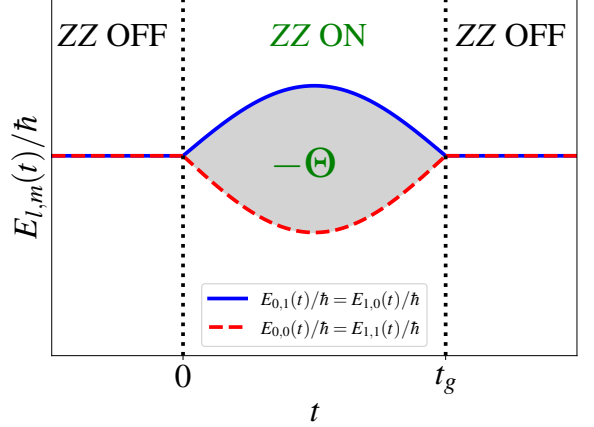


FIG. 1. A schematic of our level-degeneracy engineering to control ZZ coupling. An $R_{ZZ}(\Theta)$ gate is applied for $0 \leq t \leq t_g$. The light gray area is $-\Theta$.

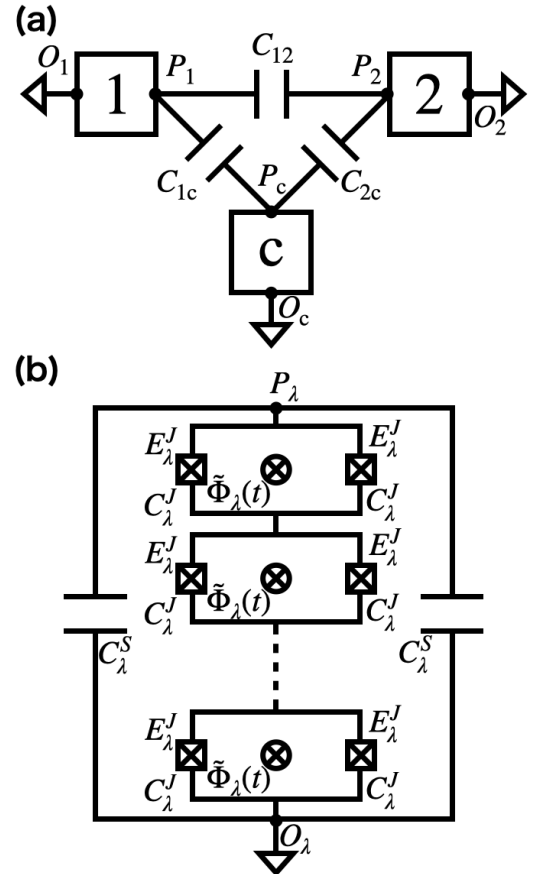


FIG. 2. A circuit model of our system, which constitutes two Kerr-cat qubits. (a) Subsystems 1, 2, and c are coupled capacitively. (b) A circuit diagram of subsystem $\lambda \in \{1, 2, c\}$, which comprises two identical shunting capacitors of capacitance C_λ^S and an array of N_λ identical symmetric dc superconducting quantum interference devices (SQUIDS) each of which has two Josephson junctions of Josephson energy E_λ^J and capacitance C_λ^J . It is connected to the ground via node O_λ . It is symmetric with respect to the line through P_λ and O_λ . The center of each SQUID is threaded by a magnetic flux $\tilde{\Phi}_\lambda(t)$ into the paper.³¹

is the reduced flux quantum [$h/(2e)$ is the flux quantum], into bias and pump parts as³²

$$\tilde{\varphi}_\lambda(t) = \tilde{\varphi}_\lambda^{\text{bias}}(t) + \tilde{\varphi}_\lambda^{\text{pump}}(t), \quad (13)$$

$$\tilde{\varphi}_\lambda^{\text{pump}}(t) = -2\pi\varepsilon_{p,\lambda} \cos(\omega_p t), \quad (14)$$

with $\varepsilon_{p,j} \ll 1$ for $j \in \{1, 2\}$ and $\varepsilon_{p,c} = 0$. In the laboratory frame, the KPOs are parametrically pumped at frequency ω_p but the resonator is not. The bias parts $\{\tilde{\varphi}_\lambda^{\text{bias}}(t)\}$ are the key components for the level-degeneracy engineering. At first, we assume that they are time independent; $\tilde{\varphi}_\lambda^{\text{bias}}(t) = \tilde{\varphi}_\lambda^{\text{bias}}(0) = \tilde{\varphi}_\lambda^{\text{bias}} \forall t$. The Hamiltonian \hat{H} of our system in a rotating frame at frequency $\omega_p/2$ under rotating-wave approximation is written as (see Sec. II in the supplementary material)

$$\hat{H} = \sum_{j=1,2} \hat{H}_j + \hat{H}_c + \hat{H}_I, \quad (15)$$

$$\hat{H}_j/\hbar = -\frac{K_j}{2}\hat{a}_j^{\dagger 2}\hat{a}_j^2 + \frac{p_j}{2}(\hat{a}_j^{\dagger 2} + \hat{a}_j^2) + \Delta_j\hat{a}_j^\dagger\hat{a}_j, \quad (16)$$

$$\hat{H}_c/\hbar = -\frac{K_c}{2}\hat{a}_c^{\dagger 2}\hat{a}_c^2 + \Delta_c\hat{a}_c^\dagger\hat{a}_c, \quad (17)$$

$$\hat{H}_I/\hbar = \sum_{j=1,2} g_{jc}(\hat{a}_j^\dagger\hat{a}_c + \hat{a}_j\hat{a}_c^\dagger) + g_{12}(\hat{a}_1^\dagger\hat{a}_2 + \hat{a}_1\hat{a}_2^\dagger), \quad (18)$$

where \hat{H}_λ is the Hamiltonian of subsystem $\lambda \in \{1, 2, c\}$ and \hat{H}_I is the beam-splitter-type interaction Hamiltonian; \hat{a}_λ is the annihilation operator of subsystem $\lambda \in \{1, 2, c\}$; K_λ is the Kerr nonlinearity of subsystem $\lambda \in \{1, 2, c\}$; p_j is the amplitude of the parametric drive of subsystem $j \in \{1, 2\}$; Δ_λ is the detuning of the dressed resonance frequency ω_λ of subsystem $\lambda \in \{1, 2, c\}$ from $\omega_p/2$, that is, $\Delta_\lambda = \omega_\lambda - \omega_p/2$; $g_{\lambda\lambda'}$ is the coupling strength between subsystems λ and λ' ($\lambda, \lambda' \in \{1, 2, c\}$). The above parameters are tuned through $\{\tilde{\varphi}_\lambda^{\text{bias}}\}$ as shown in Sec. II in the supplementary material.

Hamiltonian \hat{H} can be rewritten as

$$\hat{H} = \hat{H}_0 + \hat{H}_{ZZ} + \hat{H}_X, \quad (19)$$

$$\begin{aligned} \hat{H}_0/\hbar &= \sum_{j=1,2} \left[-\frac{K_j}{2} (\hat{a}_j^{\dagger 2} - \alpha_j^2) (\hat{a}_j^2 - \alpha_j^2) + \frac{K_j}{2} \alpha_j^4 \right] \\ &\quad + \Delta_c \left(\hat{a}_c^\dagger + \frac{g_{1c}}{\Delta_c} \hat{a}_1^\dagger + \frac{g_{2c}}{\Delta_c} \hat{a}_2^\dagger \right) \\ &\quad \times \left(\hat{a}_c + \frac{g_{1c}}{\Delta_c} \hat{a}_1 + \frac{g_{2c}}{\Delta_c} \hat{a}_2 \right), \end{aligned} \quad (20)$$

$$\hat{H}_{ZZ}/\hbar = \left(g_{12} - \frac{g_{1c}g_{2c}}{\Delta_c} \right) (\hat{a}_1^\dagger\hat{a}_2 + \hat{a}_1\hat{a}_2^\dagger) - \frac{K_c}{2}\hat{a}_c^{\dagger 2}\hat{a}_c^2, \quad (21)$$

$$\hat{H}_X/\hbar = \sum_{j=1,2} \left(\Delta_j - \frac{g_{jc}^2}{\Delta_c} \right) \hat{a}_j^\dagger\hat{a}_j, \quad (22)$$

where $\alpha_j := \sqrt{p_j/K_j}$, \hat{H}_{ZZ} is a ZZ-coupling Hamiltonian, and \hat{H}_X is a Hamiltonian for R_X gates.² In order not to apply unwanted R_X gates, we impose

$$\Delta_j - \frac{g_{jc}^2}{\Delta_c} = 0 \quad (23)$$

for $j \in \{1, 2\}$. We also set $g_{12} - g_{1c}g_{2c}/\Delta_c$, K_c , and the mean excitation number of subsystem c so small that \hat{H}_{ZZ} can be treated as a perturbation. The following tensor products of coherent states of subsystems 1, 2, and c,

$$|\psi_{0,0}\rangle := |\alpha_1, \alpha_2, -\alpha_c^+\rangle, \quad (24)$$

$$|\psi_{0,1}\rangle := |\alpha_1, -\alpha_2, -\alpha_c^-\rangle, \quad (25)$$

$$|\psi_{1,0}\rangle := |-\alpha_1, \alpha_2, \alpha_c^-\rangle, \quad (26)$$

$$|\psi_{1,1}\rangle := |-\alpha_1, -\alpha_2, \alpha_c^+\rangle, \quad (27)$$

with

$$\alpha_c^\pm = \frac{g_{1c}\alpha_1 \pm g_{2c}\alpha_2}{\Delta_c}, \quad (28)$$

are quadruply degenerate eigenstates of \hat{H}_0 with eigenenergy $E_0 = \hbar \sum_{j=1,2} K_j \alpha_j^4 / 2$. These four states are almost orthogonal since the inner product of two coherent states with opposite phases is exponentially small; $|\langle \alpha_j | -\alpha_j \rangle| = e^{-2\alpha_j^2}$. We set $\alpha_j \approx 2$ so that $|\langle \alpha_j | -\alpha_j \rangle| \approx 3 \times 10^{-4}$ for $j \in \{1, 2\}$. In the first order of perturbation, the four eigenenergies are calculated as

$$\begin{aligned} E_{0,0}/\hbar &= E_{1,1}/\hbar \\ &= E_0/\hbar + 2 \left(g_{12} - \frac{g_{1c}g_{2c}}{\Delta_c} \right) \alpha_1 \alpha_2 - \frac{K_c}{2} (\alpha_c^+)^4, \end{aligned} \quad (29)$$

$$\begin{aligned} E_{0,1}/\hbar &= E_{1,0}/\hbar \\ &= E_0/\hbar - 2 \left(g_{12} - \frac{g_{1c}g_{2c}}{\Delta_c} \right) \alpha_1 \alpha_2 - \frac{K_c}{2} (\alpha_c^-)^4. \end{aligned} \quad (30)$$

Substituting these four eigenenergies into Eqs. (3)–(6), we obtain

$$\zeta_{II} = 4E_0/\hbar - K_c \left[(\alpha_c^+)^4 + (\alpha_c^-)^4 \right], \quad (31)$$

$$\zeta_{ZZ} = 8 \left(g_{12} - \frac{g_{1c}g_{2c}}{\Delta_c} \right) \alpha_1 \alpha_2 - K_c \left[(\alpha_c^+)^4 - (\alpha_c^-)^4 \right], \quad (32)$$

and $\zeta_{IZ} = \zeta_{IZ} = 0$. We can cancel ζ_{ZZ} by regulating $\tilde{\varphi}_c^{\text{bias}}$ as in Fig. 3.

In order to check whether the above scheme for cancelling residual ZZ coupling based on the first order of perturbation is effective, we numerically calculate infidelity $1 - |\langle \Psi(t) | \Psi(0) \rangle|^2$, where $|\Psi(t)\rangle = e^{-i\hat{H}t/\hbar}|\Psi(0)\rangle$ with \hat{H} in Eq. (19) and $|\Psi(0)\rangle$ in Eq. (8) with $\beta_{0,0} = \beta_{0,1} = \beta_{1,0} = \beta_{1,1}$. For numerical calculations in this Letter, we use Quantum Toolbox in Python (QuTiP).^{33,34} Aiming to satisfy $\zeta_{ZZ} = 0$ [Eq. (32)] and Eq. (23), we choose the parameter values in Table I. We can suppress the residual coupling so that the infidelity oscillates and is less than 2×10^{-7} as in Fig. 4, about four orders of magnitude smaller than that using two tunable resonators in Ref. 29.

Next, we partially lift the level degeneracy to switch on the ZZ coupling. The bias parts $\{\tilde{\varphi}_\lambda^{\text{bias}}(t)\}$ are time dependent and so are the related parameters (see Sec. II in the supplementary

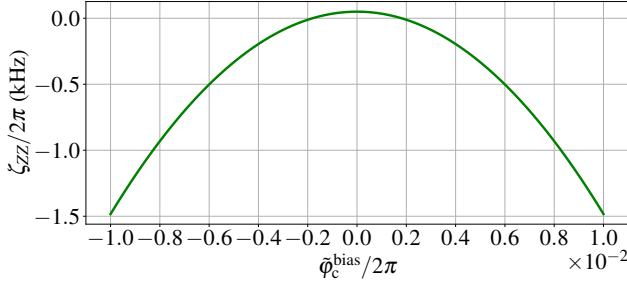


FIG. 3. ζ_{ZZ} as a function of $\tilde{\phi}_c^{\text{bias}}$. We have $\zeta_{ZZ}/2\pi = 0.0$ kHz when $\tilde{\phi}_c^{\text{bias}}/2\pi \approx \pm 2 \times 10^{-3}$. The relation between $\tilde{\phi}_c^{\text{bias}}$ and system parameters are given in Sec. II in the supplementary material. Values of the parameters unrelated to $\tilde{\phi}_c^{\text{bias}}$ are set as in Table I.

TABLE I. Parameter values chosen to satisfy $\zeta_{ZZ} = 0$ [Eq. (32)] and Eq. (23), although there is a slight deviation from Eq. (23) as in the lower right. The bold values in the left side are design values, from which the other values in the right side are calculated. The two KPOs have the same parameters. $j \in \{1, 2\}$.

C_j^S (fF)	470	$K_j/2\pi$ (MHz)	19.2
C_j^J (fF)	30	$K_c/2\pi$ (MHz)	2.58
N_j	1	$\omega_j/2\pi$ (GHz)	5.30
C_c^S (fF)	400	$\omega_c/2\pi$ (GHz)	7.26
C_c^J (fF)	30	$p_j/2\pi$ (MHz)	79.4
N_c	3	α_j	2.03
C_{12} (fF)	0.05	$g_{j_1}/2\pi$ (MHz)	23.7
C_{jc} (fF)	7	$g_{12}/2\pi$ (kHz)	287
E_j^J/h (GHz)	130	$\Delta_j/2\pi$ (kHz)	277
E_c^J/h (GHz)	426	$\Delta_c/2\pi$ (GHz)	1.96
$\tilde{\phi}_j^{\text{bias}}/2\pi$	0.25	α_c^+	0.0491
$\tilde{\phi}_c^{\text{bias}}/2\pi$	2×10^{-3}	α_c^-	0
$\varepsilon_{p,j}$	0.019	$(\Delta_j - g_{kc}^2/\Delta_c)/2\pi$ (kHz)	-10.7
$\varepsilon_{p,c}$	0		
$\omega_p/2\pi$ (GHz)	10.598944		

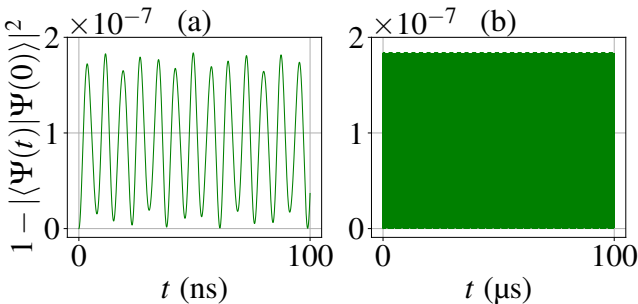


FIG. 4. Infidelity $1 - |\langle \Psi(t) | \Psi(0) \rangle|^2$ when the ZZ coupling should be switched off for (a) $0 \text{ ns} \leq t \leq 100 \text{ ns}$ and (b) $0 \mu\text{s} \leq t \leq 100 \mu\text{s}$. $|\Psi(t)\rangle = e^{-i\hat{H}t/\hbar} |\Psi(0)\rangle$ with \hat{H} in Eq. (19) and $|\Psi(0)\rangle$ in Eq. (8) with $\beta_{0,0} = \beta_{0,1} = \beta_{1,0} = \beta_{1,1}$. The used parameters are listed in Table I.

material). Though we can apply an $R_{ZZ}(\Theta)$ gate with arbitrary rotation angle Θ , we here evaluate the performance of the $R_{ZZ}(-\pi/2)$ gate. We tune $\{\tilde{\phi}_\lambda^{\text{bias}}(t)\}$ to satisfy²

$$g_{12} - \frac{g_{1c}g_{2c}}{\Delta_c(t)} = g_{12} - \frac{g_{1c}g_{2c}}{\Delta_c} - \frac{\pi^2}{16\alpha_1\alpha_2 t_g} \sin\left(\frac{\pi t}{t_g}\right) \quad (0 \leq t \leq t_g) \quad (33)$$

and the time-dependent version of Eq. (23),

$$\Delta_j(t) - \frac{g_{jc}^2}{\Delta_c(t)} = 0 \quad (34)$$

with the parameters in Table I. For example, when $t_g = 20 \text{ ns}$, $\{\Delta_\lambda(t)\}$ vary as in Fig. 5(a,b). We numerically calculate the average infidelity³⁰ of the $R_{ZZ}(-\pi/2)$ gate, $1 - \bar{F}$; see green circles in Fig. 5(c) and the supplementary material for the definition of \bar{F} . Although the infidelity oscillates with t_g , it tends to decrease with t_g for $t \lesssim 26 \text{ ns}$. We attribute this decrease to the mitigation of unwanted nonadiabatic transitions. The infidelity is less than 10^{-5} for $t_g = 25 \text{ ns}$, and about two orders of magnitude smaller than that previously reported in Ref. 29. We also consider a simpler control in which only Eq. (33) is satisfied by tuning only $\tilde{\phi}_c^{\text{bias}}(t)$. The average gate infidelity in this case corresponds to red diamonds in Fig. 5(c). Though worse than the green circles, the infidelity is less than 10^{-4} for $t_g = 25 \text{ ns}$.

In conclusion, we have proposed a ZZ-coupling scheme for two Kerr-cat qubits using a tunable resonator. By engineering the degeneracy of the four relevant states of the two Kerr-cat qubits, we can switch on and off the ZZ coupling. Our scheme is simpler and achieves smaller residual coupling and larger $R_{ZZ}(-\pi/2)$ -gate fidelity than the scheme using two tunable resonators in Ref. 29. This is because our scheme focuses on energy levels of the whole system, while the scheme in Ref. 29 focuses on those of the effective Hamiltonian of the two resonators; thus, our scheme enables more precise control of ZZ coupling. Our scheme can also be applied to superconducting nonlinear asymmetric inductive element (SNAIL)³⁵-based Kerr-cat qubits.⁶ Integrating our scheme with surface codes for biased noise^{36,37} will be an interesting future work.

SUPPLEMENTARY MATERIAL

See the supplementary material for (I) Definition of the average fidelity of the $R_{ZZ}(-\pi/2)$ gate and (II) Derivation of the system Hamiltonian.

ACKNOWLEDGMENTS

The authors are grateful to Hayato Goto for useful discussions. This Letter is based on results obtained from a project, JPNP16007, commissioned by the New Energy and Industrial Technology Development Organization (NEDO), Japan. S.M. acknowledges the support from JST [Moonshot R&D] [Grant Number JPMJMS2061].

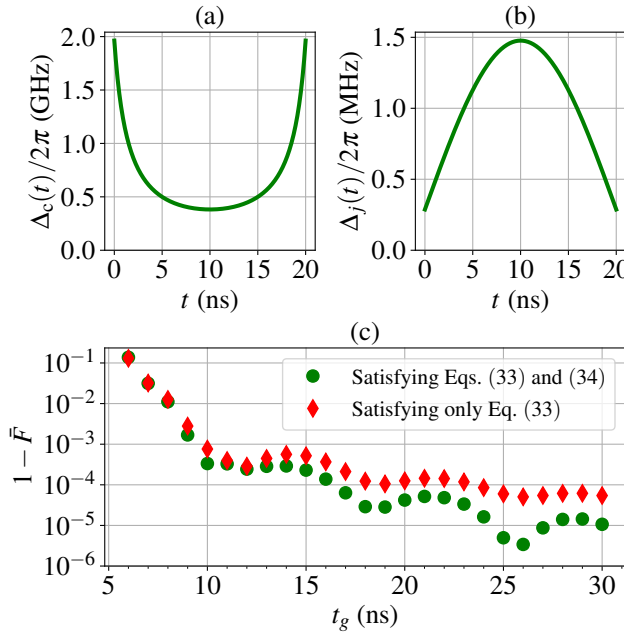


FIG. 5. (a, b) Time variations of (a) $\Delta_c(t)$ and (b) $\Delta_1(t) = \Delta_2(t)$ to satisfy Eqs. (33) and (34) when an $R_{ZZ}(-\pi/2)$ gate is performed with $t_g = 20$ ns. (c) Average infidelity of the $R_{ZZ}(-\pi/2)$ gate, $1 - \bar{F}$. The definition of \bar{F} is given in Sec. I in the supplementary material. The green circles are obtained when both of $\tilde{\phi}_c^{\text{bias}}(t)$ and $\tilde{\phi}_1^{\text{bias}}(t) = \tilde{\phi}_2^{\text{bias}}(t)$ are tuned to satisfy Eqs. (33) and (34). The red diamonds are obtained when only $\tilde{\phi}_c^{\text{bias}}(t)$ is tuned to satisfy Eq. (33); $\tilde{\phi}_j^{\text{bias}}(t) = \tilde{\phi}_j^{\text{bias}} \forall t$ for $j \in \{1, 2\}$ and Eq. (34) is not satisfied. The used parameters are listed in Table I.

AUTHOR DECLARATIONS

Conflict of Interest

The authors have no conflicts to disclose.

Author Contributions

Takaaki Aoki: Conceptualization (lead); Data curation (lead); Formal analysis (lead); Investigation (lead); Methodology (lead); Software (lead); Validation (lead); Visualization (lead); Writing – original draft (lead); Writing – review & editing (equal). **Akiyoshi Tomonaga:** Conceptualization (supporting); Data curation (supporting); Formal Analysis (supporting); Investigation (supporting); Methodology (supporting); Validation (supporting); Visualization (supporting); Writing – review & editing (equal). **Kosuke Mizuno:** Conceptualization (supporting); Data curation (supporting); Formal Analysis (supporting); Investigation (supporting); Methodology (supporting); Validation (supporting); Visualization (supporting); Writing – review & editing (equal). **Shumpei Masuda:** Conceptualization (supporting); Data curation (supporting); Formal Analysis (supporting); Investigation (supporting); Methodology (supporting); Project administration (lead); Supervision (lead); Validation (support-

ing); Visualization (supporting); Writing – original draft (supporting); Writing – review & editing (equal).

DATA AVAILABILITY

The data that support the findings of this study are available from the corresponding author upon reasonable request.

- ¹P. T. Cochrane, G. J. Milburn, and W. J. Munro, *Phys. Rev. A* **59**, 2631 (1999).
- ²H. Goto, *Phys. Rev. A* **93**, 050301 (2016).
- ³S. Puri, S. Boutin, and A. Blais, *npj Quantum Information* **3**, 18 (2017).
- ⁴S. Puri, A. Grimm, P. Campagne-Ibarcq, A. Eickbusch, K. Noh, G. Roberts, L. Jiang, M. Mirrahimi, M. H. Devoret, and S. M. Girvin, *Phys. Rev. X* **9**, 041009 (2019).
- ⁵A. S. Darmawan, B. J. Brown, A. L. Grimsmo, D. K. Tuckett, and S. Puri, *PRX Quantum* **2**, 030345 (2021).
- ⁶A. Grimm, N. E. Frattini, S. Puri, S. O. Mundhada, S. Touzard, M. Mirrahimi, S. M. Girvin, S. Shankar, and M. H. Devoret, *Nature* **584**, 205 (2020).
- ⁷T. Kanao, S. Masuda, S. Kawabata, and H. Goto, *Phys. Rev. Appl.* **18**, 014019 (2022).
- ⁸S. Masuda, T. Kanao, H. Goto, Y. Matsuzaki, T. Ishikawa, and S. Kawabata, *Phys. Rev. Appl.* **18**, 034076 (2022).
- ⁹H. Chono, T. Kanao, and H. Goto, *Phys. Rev. Res.* **4**, 043054 (2022).
- ¹⁰T. Kanao and H. Goto, *Phys. Rev. Res.* **6**, 013192 (2024).
- ¹¹S. Puri, L. St-Jean, J. A. Gross, A. Grimm, N. E. Frattini, P. S. Iyer, A. Krishna, S. Touzard, L. Jiang, A. Blais, S. T. Flammia, and S. M. Girvin, *Science Advances* **6**, eaay5901 (2020).
- ¹²Y.-H. Chen, R. Stassi, W. Qin, A. Miranowicz, and F. Nori, *Phys. Rev. Appl.* **18**, 024076 (2022).
- ¹³Q. Xu, J. K. Iverson, F. G. S. L. Brandão, and L. Jiang, *Phys. Rev. Research* **4**, 013082 (2022).
- ¹⁴D. Iyama, T. Kamiya, S. Fujii, H. Mukai, Y. Zhou, T. Nagase, A. Tomonaga, R. Wang, J.-J. Xue, S. Watabe, S. Kwon, and J.-S. Tsai, *Nature Communications* **15**, 86 (2024).
- ¹⁵M. Sarovar, T. Proctor, K. Rudinger, K. Young, E. Nielsen, and R. Blume-Kohout, *Quantum* **4**, 321 (2020).
- ¹⁶Y. Chen, C. Neill, P. Roushan, N. Leung, M. Fang, R. Barends, J. Kelly, B. Campbell, Z. Chen, B. Chiaro, A. Dunsworth, E. Jeffrey, A. Megrant, J. Y. Mutus, P. J. J. O’Malley, C. M. Quintana, D. Sank, A. Vainsencher, J. Wenner, T. C. White, M. R. Geller, A. N. Cleland, and J. M. Martinis, *Phys. Rev. Lett.* **113**, 220502 (2014).
- ¹⁷F. Yan, P. Krantz, Y. Sung, M. Kjaergaard, D. L. Campbell, T. P. Orlando, S. Gustavsson, and W. D. Oliver, *Phys. Rev. Applied* **10**, 054062 (2018).
- ¹⁸P. Mundada, G. Zhang, T. Hazard, and A. Houck, *Phys. Rev. Applied* **12**, 054023 (2019).
- ¹⁹X. Li, T. Cai, H. Yan, Z. Wang, X. Pan, Y. Ma, W. Cai, J. Han, Z. Hua, X. Han, Y. Wu, H. Zhang, H. Wang, Y. Song, L. Duan, and L. Sun, *Phys. Rev. Applied* **14**, 024070 (2020).
- ²⁰P. Zhao, P. Xu, D. Lan, J. Chu, X. Tan, H. Yu, and Y. Yu, *Phys. Rev. Lett.* **125**, 200503 (2020).
- ²¹J. Ku, X. Xu, M. Brink, D. C. McKay, J. B. Hertzberg, M. H. Ansari, and B. L. T. Plourde, *Phys. Rev. Lett.* **125**, 200504 (2020).
- ²²J. Stehlík, D. M. Zajac, D. L. Underwood, T. Phung, J. Blair, S. Carnevale, D. Klaus, G. A. Keefe, A. Carniol, M. Kumph, M. Steffen, and O. E. Dial, *Phys. Rev. Lett.* **127**, 080505 (2021).
- ²³C. Leroux, A. Di Paolo, and A. Blais, *Phys. Rev. Appl.* **16**, 064062 (2021).
- ²⁴H. Goto, *Phys. Rev. Appl.* **18**, 034038 (2022).
- ²⁵P. Zhao, K. Linghu, Z. Li, P. Xu, R. Wang, G. Xue, Y. Jin, and H. Yu, *PRX Quantum* **3**, 020301 (2022).
- ²⁶F. Marxer, A. Vepsäläinen, S. W. Jolin, J. Tuorila, A. Landra, C. Ockeloen-Korppi, W. Liu, O. Ahonen, A. Auer, L. Belzane, V. Bergholm, C. F. Chan, K. W. Chan, T. Hiltunen, J. Hotari, E. Hyypä, J. Ikonen, D. Janzso, M. Koistinen, J. Kotilahti, T. Li, J. Luus, M. Papic, M. Partanen, J. Räbinä, J. Rosti, M. Savitskyi, M. Seppälä, V. Sevriuk, E. Takala, B. Tarasinski, M. J. Thapa, F. Tosto, N. Vorobeva, L. Yu, K. Y. Tan, J. Hassel, M. Möttönen, and J. Heinsoo, *PRX Quantum* **4**, 010314 (2023).

- ²⁷K. Kubo and H. Goto, *Applied Physics Letters* **122**, 064001 (2023).
- ²⁸K. Kubo, Y. Ho, and H. Goto, *Phys. Rev. Appl.* **22**, 024057 (2024).
- ²⁹T. Aoki, T. Kanao, H. Goto, S. Kawabata, and S. Masuda, *Phys. Rev. Appl.* **21**, 014030 (2024).
- ³⁰L. H. Pedersen, N. M. Møller, and K. Mølmer, *Physics Letters A* **367**, 47 (2007).
- ³¹R. Narayan Rajmohan, A. Kenawy, and D. DiVincenzo, arXiv e-prints , arXiv:2201.01945 (2022), arXiv:2201.01945 [quant-ph].
- ³²H. Goto, *Journal of the Physical Society of Japan* **88**, 061015 (2019).
- ³³J. Johansson, P. Nation, and F. Nori, *Computer Physics Communications* **183**, 1760–1772 (2012).
- ³⁴J. Johansson, P. Nation, and F. Nori, *Computer Physics Communications* **184**, 1234–1240 (2013).
- ³⁵N. E. Frattini, U. Vool, S. Shankar, A. Narla, K. M. Sliwa, and M. H. Devoret, *Applied Physics Letters* **110**, 222603 (2017).
- ³⁶D. K. Tuckett, A. S. Darmawan, C. T. Chubb, S. Bravyi, S. D. Bartlett, and S. T. Flammia, *Phys. Rev. X* **9**, 041031 (2019).
- ³⁷J. P. Bonilla Ataides, D. K. Tuckett, S. D. Bartlett, S. T. Flammia, and B. J. Brown, *Nature Communications* **12**, 2172 (2021).

Supplemental Material: Residual-ZZ-coupling suppression and fast two-qubit gate for Kerr-cat qubits based on level-degeneracy engineering

I. Definition of the average fidelity of the $R_{ZZ}(-\pi/2)$ gate.

Average fidelity \bar{F} of the $R_{ZZ}(-\pi/2)$ gate is defined as³⁰

$$\bar{F} := \frac{\text{Tr}(\hat{M}\hat{M}^\dagger) + |\text{Tr}(\hat{M})|^2}{20}, \quad (\text{S1})$$

where $\hat{M} := [\hat{R}_{ZZ}(-\pi/2)]^\dagger \hat{U}$ with

$$\hat{U} := \sum_{l,m=0}^1 \left\langle l, \tilde{m} \right| \mathcal{T} \left[\exp \left(-\frac{i}{\hbar} \int_0^{t_g} \hat{H}(t) dt \right) \right] \left| l, \tilde{m} \right\rangle \langle \tilde{l}, \tilde{m} | \quad (\text{S2})$$

being the time-evolution operator projected on the two-qubit subspace.

II. Derivation of the system Hamiltonian

We derive the Hamiltonian of the circuit in Fig. 2 in the main text in a similar manner to Ref. 29. Upward branch flux variables across the left and right Josephson junctions of each SQUID of subsystem $\lambda \in \{1, 2, c\}$ are denoted by $\Phi_{\lambda,L}/N_\lambda$ and $\Phi_{\lambda,R}/N_\lambda$, respectively; these variables satisfy $\Phi_{\lambda,L} - \Phi_{\lambda,R} = N_\lambda \tilde{\Phi}_\lambda(t)$. Using $\Phi_\lambda := (\Phi_{\lambda,L} + \Phi_{\lambda,R})/2$, we have $\Phi_{\lambda,L} = \Phi_\lambda + N_\lambda \tilde{\Phi}_\lambda(t)/2$ and $\Phi_{\lambda,R} = \Phi_\lambda - N_\lambda \tilde{\Phi}_\lambda(t)/2$.

The kinetic energy of subsystem λ is written as

$$T_\lambda = \frac{C_\lambda^S}{2} \dot{\Phi}_{\lambda,L}^2 + \frac{C_\lambda^S}{2} \dot{\Phi}_{\lambda,R}^2 + N_\lambda \left[\frac{C_\lambda^J}{2} \left(\frac{\dot{\Phi}_{\lambda,L}}{N_\lambda} \right)^2 + \frac{C_\lambda^J}{2} \left(\frac{\dot{\Phi}_{\lambda,R}}{N_\lambda} \right)^2 \right] = \frac{C_\lambda}{2} \dot{\Phi}_\lambda^2, \quad (\text{S3})$$

where $C_\lambda := 2C_\lambda^S + 2C_\lambda^J/N_\lambda$ and we have ignored $N_\lambda C_\lambda \dot{\tilde{\Phi}}_\lambda^2/8$, which does not affect the dynamics of the system. The kinetic energy of the system is written as

$$T = \sum_{\lambda=1,2,c} T_\lambda + \frac{C_{12}}{2} (\dot{\Phi}_1 - \dot{\Phi}_2)^2 + \frac{C_{1c}}{2} (\dot{\Phi}_1 - \dot{\Phi}_c)^2 + \frac{C_{2c}}{2} (\dot{\Phi}_2 - \dot{\Phi}_c)^2 = \frac{1}{2} \dot{\Phi}^T M \dot{\Phi} = \frac{\phi_0^2}{2} \dot{\varphi}^T M \dot{\varphi}, \quad (\text{S4})$$

where

$$\Phi := \begin{pmatrix} \Phi_1 \\ \Phi_2 \\ \Phi_c \end{pmatrix}, \quad \varphi := \frac{\Phi}{\phi_0} = \begin{pmatrix} \varphi_1 \\ \varphi_2 \\ \varphi_c \end{pmatrix}, \quad \varphi_\lambda := \frac{\Phi_\lambda}{\phi_0}, \quad (\text{S5})$$

$$M = \begin{pmatrix} C_1 + C_{12} + C_{1c} & -C_{12} & -C_{1c} \\ -C_{12} & C_2 + C_{12} + C_{2c} & -C_{2c} \\ -C_{1c} & -C_{2c} & C_c + C_{1c} + C_{2c} \end{pmatrix}. \quad (\text{S6})$$

The potential energy of the system is written as

$$\begin{aligned} U(t) &= - \sum_{\lambda=1,2,c} N_\lambda \left[E_\lambda^J \cos \left(\frac{\Phi_{\lambda,L}}{N_\lambda \Phi_0} \right) + E_\lambda^J \cos \left(\frac{\Phi_{\lambda,R}}{N_\lambda \Phi_0} \right) \right] \\ &= - \sum_{\lambda=1,2,c} 2N_\lambda E_\lambda^J \cos \left(\frac{\tilde{\Phi}_\lambda(t)}{2} \right) \cos \left(\frac{\varphi_\lambda}{N_\lambda} \right), \end{aligned} \quad (\text{S7})$$

The Lagrangian of the system in the laboratory frame reads

$$\mathcal{L}(t) = T - U(t). \quad (\text{S8})$$

The conjugate momentum to $\hbar\phi_\lambda$ is denoted by n_λ and is calculated as

$$\mathbf{n} := \begin{pmatrix} n_1 \\ n_2 \\ n_c \end{pmatrix} = \frac{1}{\hbar} \frac{\partial \mathcal{L}}{\partial \dot{\varphi}} = \frac{\phi_0^2}{\hbar} M \dot{\varphi}. \quad (\text{S9})$$

Legendre transformation gives the classical Hamiltonian in the laboratory frame:

$$H^{\text{lab}}(t) = \hbar\dot{\varphi} \cdot \mathbf{n} - \mathcal{L}(t) = 2e^2 \mathbf{n}^T M^{-1} \mathbf{n} + U(t), \quad (\text{S10})$$

Since M is a symmetric matrix, M^{-1} is also symmetric, and we express $2e^2 M^{-1}$ as

$$2e^2 M^{-1} = 4 \begin{pmatrix} E_1^C & E_{12}^C & E_{1c}^C \\ E_{12}^C & E_2^C & E_{2c}^C \\ E_{1c}^C & E_{2c}^C & E_c^C \end{pmatrix}. \quad (\text{S11})$$

Quantization $n_\lambda \rightarrow \hat{n}_\lambda$ and $\varphi_\lambda \rightarrow \hat{\varphi}_\lambda$ with $[\hat{\varphi}_\lambda, \hat{n}_{\lambda'}] = i\delta_{\lambda,\lambda'}$ leads to the quantum Hamiltonian in the laboratory frame:

$$\hat{H}^{\text{lab}}(t) = \sum_{\lambda=1,2,c} \hat{H}_\lambda^{\text{lab}}(t) + \hat{H}_I^{\text{lab}}, \quad (\text{S12})$$

$$\hat{H}_\lambda^{\text{lab}}(t) = 4E_\lambda^C \hat{n}_\lambda^2 - 2N_\lambda E_\lambda^J \cos\left(\frac{\tilde{\varphi}_\lambda(t)}{2}\right) \cos\left(\frac{\hat{\varphi}_\lambda}{N_\lambda}\right), \quad (\text{S13})$$

$$\hat{H}_I^{\text{lab}} = \sum_{j=1,2} 8E_{jc}^C \hat{n}_j \hat{n}_c + 8E_{12}^C \hat{n}_1 \hat{n}_2. \quad (\text{S14})$$

We set parameters so that $E_\lambda^C \ll N_\lambda E_\lambda^J \cos(\tilde{\varphi}_\lambda(t)/2) \forall t$, which justifies expanding $\cos(\hat{\varphi}_\lambda/N_\lambda)$ to the fourth order in $\hat{\varphi}_\lambda/N_\lambda$:

$$\cos\left(\frac{\hat{\varphi}_\lambda}{N_\lambda}\right) \approx 1 - \frac{1}{2N_\lambda^2} \hat{\varphi}_\lambda^2 + \frac{1}{24N_\lambda^4} \hat{\varphi}_\lambda^4. \quad (\text{S15})$$

Since $|\varepsilon_{p,\lambda}| \ll 1$, we have

$$\cos\left(\frac{\tilde{\varphi}_\lambda(t)}{2}\right) \approx \cos\left(\frac{\tilde{\varphi}_\lambda^{\text{bias}}(t)}{2}\right) + \pi\varepsilon_{p,\lambda} \sin\left(\frac{\tilde{\varphi}_\lambda^{\text{bias}}(t)}{2}\right) \cos(\omega_p t). \quad (\text{S16})$$

Defining

$$\tilde{E}_\lambda^{J,\text{bias}}(t) := 2E_\lambda^J \cos\left(\frac{\tilde{\varphi}_\lambda^{\text{bias}}(t)}{2}\right), \quad (\text{S17})$$

$$\tilde{E}_\lambda^{J,\text{pump}}(t) := 2\pi\varepsilon_{p,\lambda} E_\lambda^J \sin\left(\frac{\tilde{\varphi}_\lambda^{\text{bias}}(t)}{2}\right) \cos(\omega_p t), \quad (\text{S18})$$

we obtain

$$\hat{H}_\lambda^{\text{lab}}(t) \approx 4E_\lambda^C \hat{n}_\lambda^2 + \frac{\tilde{E}_\lambda^{J,\text{bias}}(t)}{2N_\lambda} \hat{\varphi}_\lambda^2 + \frac{\tilde{E}_\lambda^{J,\text{pump}}(t)}{2N_\lambda} \hat{\varphi}_\lambda^2 - \frac{\tilde{E}_\lambda^{J,\text{bias}}(t)}{24N_\lambda^3} \hat{\varphi}_\lambda^4, \quad (\text{S19})$$

where we have ignored the smallest quantum-number term, $\tilde{E}_\lambda^{J,\text{pump}}(t) \hat{\varphi}_\lambda^4 / (24N_\lambda^3)$, and classical-number terms.

Inserting

$$\hat{\varphi}_\lambda = \left(\frac{2N_\lambda E_\lambda^C}{\tilde{E}_\lambda^{J,\text{bias}}(0)} \right)^{1/4} \left(\hat{a}_\lambda + \hat{a}_\lambda^\dagger \right), \quad (\text{S20})$$

$$\hat{n}_\lambda = -\frac{i}{2} \left(\frac{\tilde{E}_\lambda^{J,\text{bias}}(0)}{2N_\lambda E_\lambda^C} \right)^{1/4} \left(\hat{a}_\lambda - \hat{a}_\lambda^\dagger \right), \quad (\text{S21})$$

where \hat{a}_λ and \hat{a}_λ^\dagger are the annihilation and creation operators, into Eq. (S19) gives

$$\begin{aligned}\hat{H}_\lambda^{\text{lab}}(t)/\hbar &\approx \omega_\lambda^{(0)}(t)\hat{a}_\lambda^\dagger\hat{a}_\lambda + \frac{\omega_\lambda^{(0)}(t) - \omega_\lambda^{(0)}(0)}{2}(\hat{a}_\lambda^{\dagger 2} + \hat{a}_\lambda^2) - \frac{K_\lambda(t)}{12}(\hat{a}_\lambda + \hat{a}_\lambda^\dagger)^4 \\ &\quad + p_\lambda(t) \cos(\omega_p t) (\hat{a}_\lambda + \hat{a}_\lambda^\dagger)^2,\end{aligned}\quad (\text{S22})$$

where

$$\hbar\omega_\lambda^{(0)}(t) := \sqrt{\frac{2E_\lambda^C \tilde{E}_\lambda^{J,\text{bias}}(0)}{N_\lambda}} \left(\frac{\tilde{E}_\lambda^{J,\text{bias}}(t)}{\tilde{E}_\lambda^{J,\text{bias}}(0)} + 1 \right), \quad (\text{S23})$$

$$\hbar K_\lambda(t) := \frac{E_\lambda^C \tilde{E}_\lambda^{J,\text{bias}}(t)}{N_\lambda^2 \tilde{E}_\lambda^{J,\text{bias}}(0)}, \quad (\text{S24})$$

$$\hbar p_\lambda(t) := \pi \varepsilon_{p,\lambda} E_\lambda^J \sqrt{\frac{2E_\lambda^C}{N_\lambda \tilde{E}_\lambda^{J,\text{bias}}(0)}} \sin\left(\frac{\tilde{\varphi}_\lambda^{\text{bias}}(t)}{2}\right), \quad (\text{S25})$$

and we have omitted a classical-number term. Since the resonator does not have the pump part of the dimensionless magnetic flux, $\varepsilon_{p,c} = 0$, we have $p_c(t) = 0 \forall t$. Substituting Eq. (S21) into Eq. (S14) leads to

$$\hat{H}_{\text{I}}^{\text{lab}}/\hbar = - \sum_{j=1}^2 g_{jc} (\hat{a}_j - \hat{a}_j^\dagger) (\hat{a}_c - \hat{a}_c^\dagger) - g_{12} (\hat{a}_1 - \hat{a}_1^\dagger) (\hat{a}_2 - \hat{a}_2^\dagger) \quad (\text{S26})$$

where

$$\hbar g_{jc} = \sqrt{2} E_{jc}^C \left(\frac{\tilde{E}_j^{J,\text{bias}}(0) \tilde{E}_c^{J,\text{bias}}(0)}{N_j N_c E_j^C E_c^C} \right)^{1/4}, \quad \hbar g_{12} = \sqrt{2} E_{12}^C \left(\frac{\tilde{E}_1^{J,\text{bias}}(0) \tilde{E}_2^{J,\text{bias}}(0)}{N_1 N_2 E_1^C E_2^C} \right)^{1/4}. \quad (\text{S27})$$

Moving on to a rotating frame at frequency $\omega_p/2$ and ignoring rapidly oscillating terms (rotating-wave approximation), the Hamiltonian of the system can be written as

$$\hat{H}(t) = \hat{R}(t) \hat{H}^{\text{lab}}(t) \hat{R}^\dagger(t) + i\hbar \frac{d\hat{R}(t)}{dt} \hat{R}^\dagger(t) = \sum_{j=1,2} \hat{H}_j(t) + \hat{H}_c(t) + \hat{H}_{\text{I}}, \quad (\text{S28})$$

where

$$\hat{R}(t) = \exp \left[i \frac{\omega_p}{2} t \sum_{\lambda=1,2,c} \hat{a}_\lambda^\dagger \hat{a}_\lambda \right], \quad (\text{S29})$$

$$\hat{H}_j(t)/\hbar = -\frac{K_j(t)}{2} \hat{a}_j^{\dagger 2} \hat{a}_j^2 + \frac{p_j(t)}{2} (\hat{a}_j^{\dagger 2} + \hat{a}_j^2) + \Delta_j(t) \hat{a}_j^\dagger \hat{a}_j, \quad (\text{S30})$$

$$\hat{H}_c(t)/\hbar = -\frac{K_c(t)}{2} \hat{a}_c^{\dagger 2} \hat{a}_c^2 + \Delta_c(t) \hat{a}_c^\dagger \hat{a}_c, \quad (\text{S31})$$

$$\hat{H}_{\text{I}}/\hbar = \sum_{j=1,2} g_{jc} (\hat{a}_j^\dagger \hat{a}_c + \hat{a}_j \hat{a}_c^\dagger) + g_{12} (\hat{a}_1^\dagger \hat{a}_2 + \hat{a}_1 \hat{a}_2^\dagger), \quad (\text{S32})$$

with $\Delta_\lambda(t) := \omega_\lambda(t) - \omega_p/2$ and $\omega_\lambda(t) := \omega_\lambda^{(0)}(t) - K_\lambda(t)$.